Genetic algorithms for 3D reconstruction with supershapes

4 authors, including:

Sophie Voisin
Oak Ridge National Laboratory
30 PUBLICATIONS **558** CITATIONS

SEE PROFILE

Frederic Truchetet
University of Burgundy
236 PUBLICATIONS **2,166** CITATIONS

SEE PROFILE

GENETIC ALGORITHMS FOR 3D RECONSTRUCTION WITH SUPERSHAPES

S. Voisin*, *M. A. Abidi*†

IRIS Laboratory
The University of Tennessee
Elect. Eng. and Comp. Sc. Department
Knoxville, TN, USA

S. Foufou, F. Truchetet

Laboratoire LE2I - UMR CNRS 5158
Université de Bourgogne
Département d'Informatique
Dijon, France

ABSTRACT

Supershape model is a recent primitive that represents numerous 3D shapes with several symmetry axes. The main interest of this model is its capability to reconstruct more complex shape than superquadric model with only one implicit equation. In this paper we propose a genetic algorithms to reconstruct a point cloud using those primitives. We used the pseudo-Euclidean distance to introduce a threshold to handle real data imperfection and speed up the process. Simulations using our proposed fitness functions and a fitness function based on inside-outside function show that our fitness function based on the pseudo-Euclidean distance performs better.

Index Terms— 3D Reconstruction, genetic algorithms, supershapes, pseudo-Euclidean distance

1. INTRODUCTION

3D point cloud reconstruction with methods based on parametric surface fitting is an important field of investigation in image processing. Among those methods, superquadric model [1] have been very well studied [2-15], when methods based on the recent supershape model [16] have been barely investigating [17, 18]. Although an analogy between superquadric and supershape models can be made, and that optimization methods to recover the parameters of the best superquadric fitting are usually based on the Levenberg-Marquardt (LM) theory [19], LM cannot be applied to retrieve all the parameters for supershape fitting. Indeed, the symmetry parameters of the supershape model have to be integers in order to obtain a meaningful inside-outside functions (closed primitives), leading to consider discontinuous functions that cannot be used by the LM approach. In this paper, we propose a method based on Genetic Algorithm (GAs) [20] in order 1) to overcome the problem of discontinuity; and 2) to avoid initialization problems that may occur when using deterministic approaches.

GAs have been already studied for supershapes [18]. However, we found their fitness function based on inside-outside function not suitable to real data where accuracy has to be sacrificed in favor of a tolerance threshold that will handle the presence of noise. Therefore, we use the pseudo-Euclidean distance to evaluate the solution and to integrate
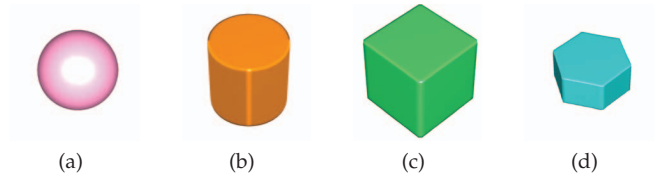
Fig. 1. Shapes examples.

Table 1. Supershapes parameters

Figure	m	n_1, n_2, n_3	M	N_1, N_2, N_3	s_x, s_y, s_z
1(a)	4	2, 2, 2	4	2, 2, 2	5, 5, 5
1(b)	4	2, 2, 2	4	100, 100, 100	5, 5, 5
1(c)	4	100, 100, 100	4	100, 100, 100	5, 5, 5
1(d)	6	100, 45, 45	4	100, 100, 100	5, 5, 2.5

this threshold. We have also noticed that for synthetic data, the computation time of GAs can be improved using an initial population that contains some particular individuals, known primitives with specific scale, position, and orientation. However, when real data has to be reconstructed this initialization is not competitive anymore. Therefore, we introduce a constraint that penalizes some individuals during the process to invalidate inappropriate solutions either with synthetic or real data.

In the following, firstly, we present the supershape model that we use as primitive to reconstruct the point cloud. Secondly, we propose our method combining GAs, a fitness function based on the pseudo-Euclidean distance, and integrating a threshold to address noise issue and speeds up the overall process. Thirdly, we give preliminary results of our method and compare its performance to GAs methods using the fitness based on inside-outside function. Finally, we conclude on the performance of our method and give idea on future work.

2. SUPERSHAPES

Among the different object representations we have chosen to explore the supershape model that have been introduced six years ago by Gielis [16] as an extension of superquadrics. The main advantage of this model resides in its two symmetry parameters m and M, allowing to generate more complex shapes

than superquadric model. Therefore, it is possible to reconstruct the same objects as superquadric model as well as objects with more than four symmetry axes, see Fig. 1 and Tab. 1. Supershapes are the result of the spherical product between two generalized superellipses, as described by equations 1, 2, and 3:

$$\vec{s}\,(\eta,\omega) = \begin{pmatrix} x(\eta,\omega) \\ y(\eta,\omega) \\ z(\eta,\omega) \end{pmatrix} = \begin{pmatrix} r_1(\eta)r_2(\omega)\cos(\eta)\cos(\omega) \\ r_1(\eta)r_2(\omega)\sin(\eta)\cos(\omega) \\ r_2(\omega)\sin(\omega) \end{pmatrix} \quad (1)$$

$$r_1(\eta) = \left(\left| \frac{1}{a}\cos\left(\frac{m\eta}{4}\right) \right|^{n_2} + \left| \frac{1}{b}\sin\left(\frac{m\eta}{4}\right) \right|^{n_3} \right)^{-\frac{1}{n_1}} \quad (2)$$

$$r_2(\omega) = \left(\left| \frac{1}{a}\cos\left(\frac{M\omega}{4}\right) \right|^{N_2} + \left| \frac{1}{b}\sin\left(\frac{M\omega}{4}\right) \right|^{N_3} \right)^{-\frac{1}{N_1}} \quad (3)$$

where $-\pi \leq \eta < \pi$ and $-\frac{\pi}{2} \leq \omega < \frac{\pi}{2}$, a, b, n_i, and $N_i \in \mathbb{R}^+$ and m, and $M \in \mathbb{R}^+_*$. Notice that in our study we have considered the unitary supershapes, *i.e.* $a = b = 1$.

In addition, supershapes can be also represented by an inside-outside function as mention in [17]:

$$F(x,y,z) = \frac{x^2 + y^2 + z^2}{r_1^2(\eta)r_2^2(\omega)} = \frac{\|\overrightarrow{OP}\|}{\|\overrightarrow{OI}\|} = 1 \quad (4)$$

where O is the center of the supershape, $P(x,y,z)$ is the point in 3D space, and $I(x_I, y_I, z_I)$ is its corresponding point on the surface. Notice that I is the intersection point between the ray OP and the supershape and it is computed using Eq. 1 and the following:

$$\eta = \tan^{-1}\left(\frac{x}{y}\right) \quad (5)$$

$$\omega = \tan^{-1}\left(\frac{z \cdot r_1(\eta) \cdot \sin(\eta)}{y}\right) = \tan^{-1}\left(\frac{z \cdot r_1(\eta) \cdot \cos(\eta)}{x}\right) \quad (6)$$

Because the primitives are defined at the origin of the world frame, we have also to consider the transformations that modify the unitary superquadric. First the scaling $S(s_x, s_y, s_z)$, then the rotations of the axes $R(\theta, \phi, \psi)$, and finally the translation $T(d_x, d_y, d_z)$ are applied for the placement of the parametric surface in the world frame coordinate. This implies that 17 parameters (m, n_1, n_2, n_3, M, N_1, N_2, N_3, s_x, s_y, s_z, θ, ϕ, ψ, d_x, d_y, d_z) have to be retrieved for reconstruction based on supershape fitting.

3. FITTING ERROR ANALYSIS

In the superquadric literature, several studies such as [13, 14, 15] compare different fitting errors. When the conclusion in [13] is in favor of an error based on pseudo-Euclidean distance, the two others conclude that the inside-outside function may perform better depending on the type of application and data. That may explain the preference of numerous authors such as [2-9] for fitting errors based on the inside-outside function. We have also noticed that [17, 18] use the inside-outside function for their reconstruction methods based on supershape fitting. However, because real data is noisy and often contains errors from image processing (registration and integration), we have decided to base our fitting error on the

pseudo-Euclidean distance, $D(P_i, \mathcal{S}) = \|I_i P_i\|$, which is the distance between P_i in the point cloud and its corresponding point I_i on the surface $\mathcal{S}$. This allows us to integrate a tolerance threshold τ in order to compensate for noise and errors and to make our method more robust. Therefore we consider the following equation:

$$Eof_1^\tau(\mathcal{S}) = \frac{1}{\mathcal{N}} \sum_{i=1}^{\mathcal{N}} D^\tau(P_i, \mathcal{S}) \quad (7)$$

$$D^\tau(P_i, \mathcal{S}) = \begin{cases} D(P_i, \mathcal{S}) = \|I_i P_i\| & \text{if } D(P_i, \mathcal{S}) > \tau \\ 0 & \text{otherwise} \end{cases} \quad (8)$$

This basically means that, for every point within the threshold, the parametric surface is considered as a perfect fit and the value of $\|I_i P_i\|$ is set to 0, i.e., a fitting error equal to 0 corresponds to the perfect fit with respect to the threshold τ.

Considering the LM method initialization, we have noticed that most of the time the initial shape is a sphere placed inside the point cloud. We formulate this property with a constraint on the scalar product between each normal at the point P and its corresponding point I on the surface to penalize the supershapes that have not their center inside the point cloud. Therefore we use the following fitting error:

$$Eof_1 = \begin{cases} n_{rev} & \text{if } \exists\, i \text{ such as } \langle n_{I_i} \cdot n_{P_i} \rangle < 0 \\ Eof_1^\tau(\mathcal{S}) & \text{otherwise} \end{cases} \quad (9)$$

where n_{rev} is the number of points that penalize the supershape $\mathcal{S}$, the points P_i and I_i have been already described, and have the respective normal n_{P_i} and n_{I_i} ($nx_{I_i}, ny_{I_i}, nz_{I_i}$), this latter is computed from:

$$nx_{I_i} = r_2(\omega)\cos\omega\,[r_1'(\eta)\cos\eta - r_1(\eta)\sin\eta] + \\ r_1(\eta)\cos\eta\,[r_2'(\omega)\cos\omega - r_2(\omega)\sin\omega] \quad (10)$$

$$ny_{I_i} = r_2(\omega)\cos\omega\,[r_1'(\eta)\sin\theta + r_1(\eta)\cos\eta] + \\ r_1(\eta)\sin\eta\,[r_2'(\omega)\cos\omega - r_2(\omega)\sin\omega] \quad (11)$$

$$nz_{I_i} = r_2'(\omega)\sin\omega + r_2(\omega)\cos\omega \quad (12)$$

with η and ω from Equations 5 and 6.

Therefore the reconstruction problem is defined as the following minimization problem:

$$\min\left(Eof_1\left(\mathcal{S} : m, n_{1..3}, M, N_{1..3}, s_x, s_y, s_z, \theta, \phi, \psi, d_x, d_y, d_z\right)\right) \quad (13)$$

4. GENETIC ALGORITHMS STRATEGIES

To solve the optimization problem that we just describe, we implement a GAs method that follows the classic scheme, Fig. 2. We *encode* the solution with a real value, limit and sample each domain to obtain a meaningful values of the parameters. Each generation is composed of a *population* that contains 5000 individuals. The *selection* method randomly chooses both parents. The *crossover* mixes them following the uniform exchange of each gene. The *mutation* is applied to a quarter of the population and randomly replaces one or two genes of the chromosome. This subsequently keeps the diversity of the genetic material. The genes values are randomly replaced with values in the corresponding parameter
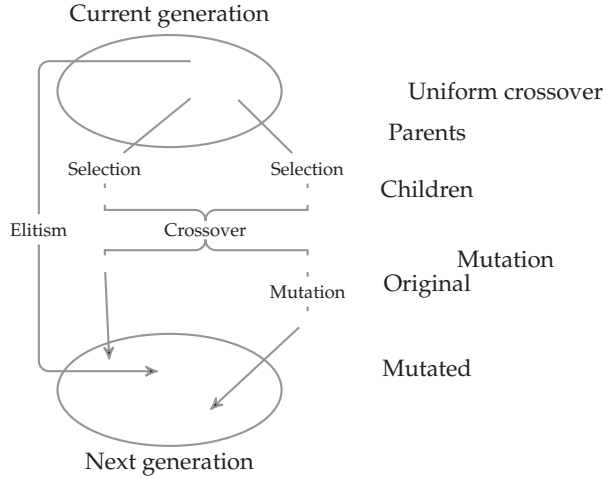
Fig. 2. The GAs strategies: the random selection, the crossover using uniform exchange, the mutation, and the elitism.

domains. ***Elitism*** keeps a small percentage of the best individuals from one generation to the next. We have implemented three different ***stopping criteria***. The first one is a threshold under which the fitness value is considered acceptable. Indeed, it is almost impossible to have the fitness equal to 0 due to computation approximation and/or noise. The second stopping criterion is the fact that all elites are identical. This phenomenon means that the algorithm reaches a family of solutions, either local or global, and that the genetic material does not allow for the exploration of more solutions. The last stopping criterion is the maximum number of generations allowed. Finally to evaluate the individuals we use the fitting error described Eq. 15 as ***fitness function***.

5. RESULTS

We have compared our GAs method using the fitness function Eof_1 to the same GAs method using the fitness function Eof_2 based on the inside-outside function from [18]:

$$Eof_2 = s_x s_y s_z \sum_{i=1}^{\mathcal{N}} \left(F\left(P_i \right) - 1 \right)^2 \quad (14)$$

where $F\left(P_i \right)$ is given Eq. 4, s_x, s_y, and s_z are the scale factor with respect to the three axes x-, y- and z-. We observe that GAs with Eof_2 as it is described in [18] is sensitive to misclassification of the best individuals if we have to consider scales below one unit.

We also test the inside-outside function with a threshold and similar constraint than Eof_1:

$$Eof_3 = \begin{cases} n_{rev} & \text{if } \exists\, i \text{ such as } \langle n_{I_i} \cdot n_{P_i} \rangle < 0 \\ Eof_3^{\tau}\left(\mathcal{S} \right) & \text{otherwise} \end{cases} \quad (15)$$

$$Eof_3^{\tau}\left(\mathcal{S} \right) = \frac{1}{\mathcal{N}} \sum_{i=1}^{\mathcal{N}} F^{\tau}\left(P_i, \mathcal{S} \right) \quad (16)$$

$$F^{\tau}\left(P_i, \mathcal{S} \right) = \begin{cases} F\left(P_i, \mathcal{S} \right) = |F\left(P_i \right) - 1| & \text{if } F\left(P_i, \mathcal{S} \right) > \tau \\ 0 & \text{otherwise} \end{cases} \quad (17)$$

As we expected, we could observe that the parametric surface becomes increasingly further away from the ideal solution as the threshold increases, Figures 3(d), 3(e), and 3(f). In addition we noticed interesting behavior, as the threshold becomes equal or superior to 1. These thresholds lead to an immediate solution with a fitness value equal to 0, which represents any parametric surface that contains the point cloud. This behavior can be explained by the distribution of the inside-outside function that have a maximum equals to 1 at the center of the supershape. Therefore, Eof_1 seems to be the most adapted to use GAs optimization method. The function analysis does not show any problem for us to use it as fitness function.

6. CONCLUSION

We describe a GAs method for 3D reconstruction using a fitness function based on the pseudo-Euclidean distance that integrate a tolerance threshold to handle noisy data. We have added a constraint on the parametric surface center to penalize some solutions in accordance of deterministic method initialization. The proposed fitness function with the constraints met our expectations and experimentations on several data have shown that it performs better than the GAs method using the inside-outside function and that it is not sensitive to initialization such as LM method. This method can be also generalized to other primitive models such as superquadrics.

7. REFERENCES

[1] A.H. Barr, "Superquadrics and Angle-Preserving Transformations," *Computer Graphics and Applications IEEE*, vol. 1, no. 1, pp. 11–23, January 1981.

[2] A. Gupta and R. Bajcsy, "Volumetric Segmentation of Range Images of 3D Objects Using Superquadrics Models," *Computer Vision, Graphics and Image Processing: Image Understanding, CVGIP*, vol. 58, no. 3, pp. 302–326, November 1993.

[3] A. Gupta, L. Bogoni, and R. Bajcsy, "Quantitative and Qualitative Measures for the Evaluation of the Superquadric Models," in *Interpretation of 3D Scenes Workshop on*, Austin, Texas, USA, November 1989, pp. 162–169.

[4] A. Jaklič, A. Leonardis, and F. Solina, *Segmentation and Recovery of Superquadrics*, Kluwer Academic Publishers, Dordrecht, Boston, London, 2000.

[5] F. Solina and R. Bajcsy, "Recovery of Parametric Models from Range Images: The Case for Sperquadrics with Global Deformations," *IEEE Transactions on Pattern Analysis and Machine Intelligence*, vol. 12, no. 2, pp. 131–147, February 1990.

[6] E. Bardinet, L.D. Cohen, and N. Ayache, "Fitting of Iso-Surfaces Using Superquadrics and Free-Form Deformations," in *Proceedings of the IEEE Workshop on Biomedical Image Analysis*, Seattle, Washington, USA, June 1994, pp. 184–193.

[7] E. Bardinet, L.D. Cohen, and N. Ayache, "Fitting 3-D Data Using Superquadrics and Free-Form Deformations," in *Proceedings of the 12th IAPR International Conference on Pattern Recognition, Conference A: Computer Vision*

| | (a) | (b) | (c) | (d) | (e) | (f) |
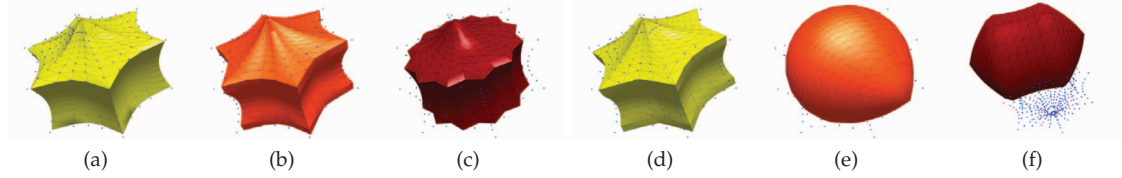
Fig. 3. Visual results for the fitness functions Eof_1 (3(a) to 3(c)), and Eof_3 (3(d) to 3(f)): hexagonal shape. The parameters of each results are given Tab. 2.

Table 2. This tables relates the results for a synthetic shapes and the visual results are given Fig 3. The $*$ indicates the simulation ending with criterion: the maximum number of iteration has been reached.

						Eof_1						
$\tau_{\mathcal{D}}$	Fig.	m	n_1, n_2, n_3	M	N_1, N_2, N_3	s_x, s_y, s_z	θ, ϕ, ψ	d_x, d_y, d_z	Points	Fitness	Iteration
0.1	3(a)	6	48, 48, 50	6	45, 36, 42	5.2, 5.2, 5	0, 0, 180	-0.1, 0, 0	391	0.009	1000*
0.5	3(b)	6	24, 23, 31	6	23, 28, 16	4.9, 5.1, 5.4	1, 180, 1	-0.1, 0, 0	573	0.005	822
1	3(c)	12	14, 36, 5	6	38, 27, 32	5.5, 5.5, 5.2	1, 1, 16	0, -0.1, -0.1	573	0.009	1587
						Eof_2						
$\tau_{\mathcal{D}}$	Fig.	m	n_1, n_2, n_3	M	N_1, N_2, N_3	s_x, s_y, s_z	θ, ϕ, ψ	d_x, d_y, d_z	Points	Fitness	Iteration
n/a	n/a	1	1, 81, 86	1	1, 61, 56	0.1, 0.1, 0.1	104, 49, 99	7, -8.4, 6.2	n/a	0.044.	500*
						Eof_3						
$\tau_{\mathcal{D}}$	Fig.	m	n_1, n_2, n_3	M	N_1, N_2, N_3	s_x, s_y, s_z	θ, ϕ, ψ	d_x, d_y, d_z	Points	Fitness	Iteration
0.1	3(d)	6	25, 33, 24	6	29, 30, 19	5.1, 5.2, 5.4	180, 3, 62	-0.2, -0.1, -0.1	535	0.009	821
0.5	3(e)	2	39, 17, 4	2	10, 18, 36	7.8, 6.7, 4.9	98, 27, 32	-0.5, -0.7, -0.1	570	0.007	24
1	3(f)	6	25, 39, 3	6	47, 35, 13	6.3, 9.2, 10.8	120, 85, 104	0.7, -6.2, 6.6	578	0	1

and Image Processing, Jerusalem, Israel, October 1994, pp. 79–83.

[8] D. Katsoulas, "Reliable Recovery of Piled Box-like Objects via Parabolically Deformable Superquadrics," in *Proceedings of the Ninth IEEE International Conference on Computer Vision ICCV'03*, Nice, France, October 2003, pp. 931–938.

[9] F.P. Ferrie, J. Lagarde, and P. Whaite, "Darboux Frames, Snakes, and Super-Quadrics: Geometry from the Bottom Up," *IEEE Transactions on Pattern Analysis and Machine Intelligence*, vol. 15, no. 8, pp. 771–784, August 1993.

[10] C.T. Lim, G.M. Turkiyyah, M.A. Ganter, and D.W. Storti, "Implicit Reconstruction of Solids from Cloud Point Sets," in *the third ACM Symposium on Solid Modeling and Applications*, Salt Lake City, Utah, USA, 1995, pp. 393–402.

[11] D. Terzopoulos and D. Metaxas, "Dynamic 3D Models with Local and Global Deformations: Deformable Superquadrics," *IEEE Transactions on Pattern Analysis and Machine Intelligence*, vol. 13, no. 7, pp. 703–714, July 1991.

[12] H. Saito and N. Tsunashima, "Estimation of 3-D Parametric Models from Shading Image Using Genetic Algorithms," in *IEEE 12th International Conference on Pattern Recognition*, Jerusalem, Israel, October 1994, pp. 668–670.

[13] A.D. Gross and T.E. Boult, "Error of Fit Measures for Recovering Parametric Solids," in *Proceedings of the Second International Conference in Computer Vision*, Tampa, Florida, USA, December 1988, pp. 690–694.

[14] E.R. van Dop and P.P.L. Regtien, "Fitting underformed superquadrics to range data: improving model recov-

ery and classification," in *Computer Vision and Pattern Recognition*, Santa Barbara, California, USA, June 1998, pp. 396–401.

[15] Y. Zhang, "Experimental comparison of superquadric fitting objective functions," *Pattern Recognition Letters*, vol. 24, pp. 2185–2193, 2003.

[16] J. Gielis, "A Generic Geometric Transformation that Unifies a Wide Range of Natural and Abstract Shapes," *American Journal of Botany*, vol. 90, no. 3, pp. 333–338, 2003.

[17] Y.D. Fougerolle, A. Gribok, S. Foufou, F. Truchetet, and M.A. Abidi, "Supershape Recovery from 3D Data Sets," in *IEEE International Conference on Image Processing ICIP2006*, Atlanta, Georgia, USA, October 2006, pp. 2193–2196.

[18] Y. Bokhabrine, Y.D. Fougerolle, S. Foufou, and F. Truchetet, "Genetic Algorithms for Gielis Surface Recovery from 3D Data Sets," *IEEE International Conference on Image Processing ICIP*, September 2007.

[19] W.H. Press, S.A. Teukolsky, W.T. Vetterling, and B.P. Flannery, *Numerical Recipes in C: The Art of Scientific Computing Second Edition*, Cambridge University Press, 1992.

[20] J.H. Holland, *Adaptation in natural and artificial systems : an introductory analysis with applications to biology, control, and artificial intelligence*, Ann Arbor : University of Michigan, 1975.